Cell Reports, Volume *30*

Supplemental Information

BMP Signaling Gradient Scaling

in the Zebrafish Pectoral Fin

Rita Mateus, Laurent Holtzer, Carole Seum, Zena Hadjivasiliou, Marine Dubois, Frank Jülicher, and Marcos Gonzalez-Gaitan

Supplemental Figures

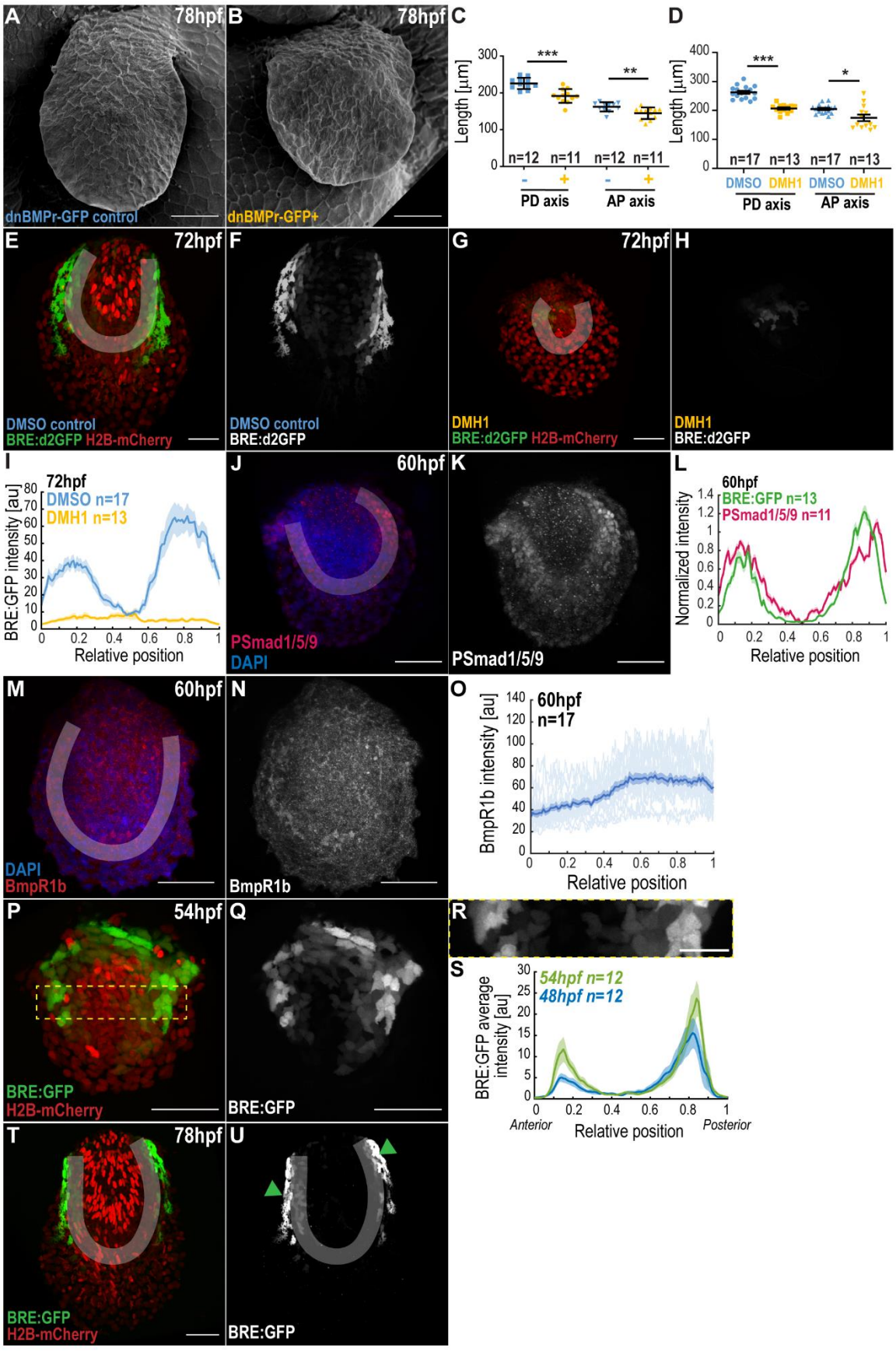

Figure S1. Characterization of BRE:GFP signalling gradients. Related to Figure 1.
A-I Inhibition of BMP signalling leads to fin growth defects. **A-B** SEM of fins expressing dominant negative BMP receptor in transgenic fish (dnBmpr-GFP+, B) or in sibling controls (A), at 78 hpf (for heat-shock conditions, see STAR Methods). **C** Average PD and AP lengths of fins in conditions as in A-B. **D** Average PD and AP lengths of fins of conditions as in E-H. Mean ± s.e.m. are shown in all bar graphs. For all statistical analyses: ***P<0.0001; **P<0.01; *P<0.05; two-tailed, unpaired, non-parametric Mann–Whitney tests. **E-H** Live imaging of BRE:d2GFP; H2B-mCherry transgenics, in DMH1-treated (G-H) and control larvae (E-F), at 72 hpf (for inhibitor conditions, see STAR Methods). **I** Average intensity of BRE:GFP signal *versus* relative position (ROI midline) in DMH1-treated (yellow) and control larvae (blue), in conditions as in E-H. **J-K** Phospho-Smad1/5/9 immunostaining (red) and DAPI (blue), at 60 hpf. **L** Comparison between average intensities of normalized Phospho-Smad1/5/9 (red, from immunostaining) and BRE:GFP (green, from live imaging) versus relative position (ROI midline). **M-N** Bmp receptor 1b immunostaining (red) and DAPI (blue), at 60 hpf. **O** Average intensity of BmpR1b signal versus relative position (ROI midline). **P-Q** Fin of double transgenic BRE:GFP (green) and Histone2b-mCherry (red) at 54 hpf. Dash outline delimits the AP ROI used for quantification. **R** Cropped BRE:GFP gradient along the AP ROI from P. **S** Average intensity of BRE:GFP signal *versus* relative position (AP ROI), at 48 and 54 hpf. **T-U** Live imaging of BRE:GFP (green); H2B-mCherry transgenics (red), at 78 hpf. Note that at 78 hpf (and later, not shown) BRE:GFP drives high levels of expression in individual cells (arrowheads) in the fin fold adjacent to the endoskeletal disc in a pattern different to the gradient considered in this study. All shadowing in graphs, s.e.m. per relative position. n represents number of fins analysed. All fin images: anterior, left; distal, down. Region of interest (ROI midline), white highlight. BRE:GFP transgene used: BRE:d2GFP (Collery and Link, 2011) (E-I); BRE:eGFP (Laux et al., 2011) (L-P, T-U). Scale bars, 50µm (A-B, E,G,J-K, M-N, P-R, T); 20µm (R).

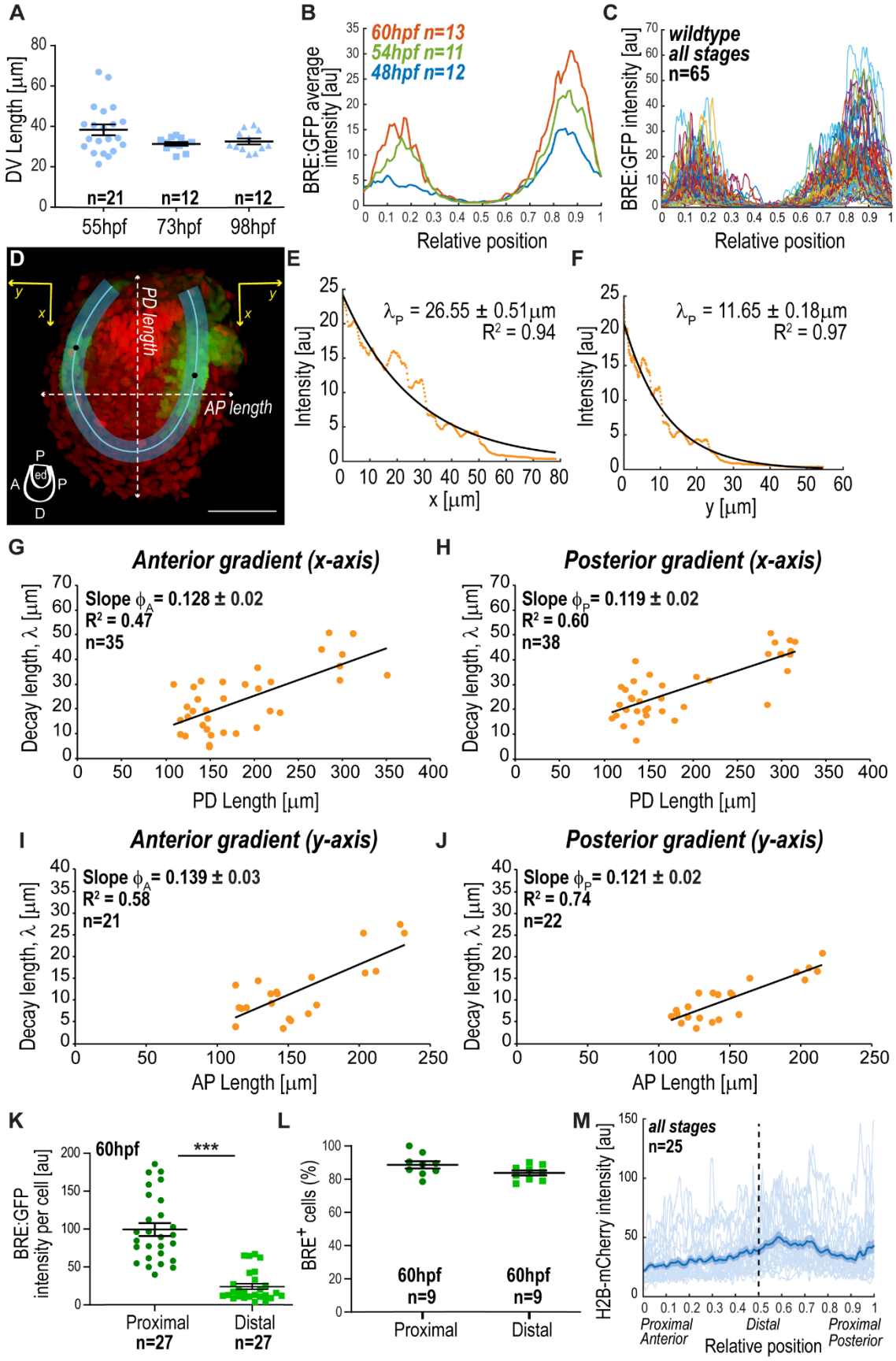
A
DV Length [µm]
n=21
n=12
n=12
55hpf
73hpf
98hpf
B
60hpf n=13
54hpf n=11
48hpf n=12
BRE:GFP average intensity [au]
Relative position
C
wildtype
all stages
n=65
BRE:GFP intensity [au]
Relative position
D
PD length
AP length
y
x
P
A
ed
D
E
λP = 26.55 ± 0.51µm
R2 = 0.94
Intensity [au]
x [µm]
F
λP = 11.65 ± 0.18µm
R2 = 0.97
Intensity [au]
y [µm]
G
Anterior gradient (x-axis)
Slope ϕA = 0.128 ± 0.02
R2 = 0.47
n=35
Decay length, λ [µm]
PD Length [µm]
H
Posterior gradient (x-axis)
Slope ϕP = 0.119 ± 0.02
R2 = 0.60
n=38
Decay length, λ [µm]
PD Length [µm]
I
Anterior gradient (y-axis)
Slope ϕA = 0.139 ± 0.03
R2 = 0.58
n=21
Decay length, λ [µm]
AP Length [µm]
J
Posterior gradient (y-axis)
Slope ϕP = 0.121 ± 0.02
R2 = 0.74
n=22
Decay length, λ [µm]
AP Length [µm]
K
60hpf
***
BRE:GFP intensity per cell [au]
Proximal
n=27
Distal
n=27
L
BRE+ cells (%)
60hpf
n=9
60hpf
n=9
Proximal
Distal
M
all stages
n=25
H2B-mCherry intensity [au]
Proximal Anterior
Distal
Proximal Posterior
Relative position

Figure S2. Cartesian system to measure the gradients and scaling. Related to Figures 1 and 3.

A DV fin lengths (from live imaging of H2B-mCherry transgenics), at different developmental stages. Note that there is no growth along the DV axis in the stages considered in this study. **B** Average intensities of BRE:GFP at different developmental stages *versus* relative position (ROI midline). **C** Intensity of individual BRE:GFP profiles *versus* relative position (ROI midline) from 48 to 78 hpf. **D** Fin of double transgenic BRE:GFP (green) and Histone2b-mCherry (red) from Fig. 1A. Region of interest (ROI), with midline (blue). PD length, distance between the proximal base of the fin and its distal tip along the PD axis. AP length, distance between the anterior-most part of the fin to its posterior-most position (white lines). Cartoon indicates fin axes and endoskeletal disc (ed). Scale bar, 50µm. **E-F** BRE:GFP intensity profiles versus *x* (E) or *y* (F) position for the posterior gradient in D, with respective decay lengths (λ, slope), ± s.e.m. Here $x = 0$ (E) or $y = 0$ (F), position of peak signal as indicated in D (black dots). Black lines, exponential fits with respective goodness of fit (R^2). **G-J** Decay lengths λ from exponential fits obtained from BRE:GFP intensity profiles in *x versus* PD length (G-H) or in *y versus* AP length (I-J). Slope (ϕ) values ± s.e.m. are shown. Lines, linear fits with goodness of fit (R^2). **K-M** Gradient signalling levels decrease along ROI midline, at 60 hpf. **K** Comparison between BRE:GFP average intensity per cell in proximal and distal areas of the gradient. **L** Comparison between the percentage of H2B-mCherry positive cells which are positive for BRE:GFP in proximal and distal areas of the gradient. **M** Nuclear density measured by H2B-mCherry signal along the ROI midline, showing that cell density is approximately homogeneous along the endoskeletal disc. Light blue, individual fin profiles; dark blue line, average intensity; shadowing, s.e.m. per relative position. Black dash indicates the most distal position in ROI, where density is similar to proximal positions. For all statistical analyses: ***P<0.0001; two-tailed, unpaired, non-parametric Mann–Whitney tests. Mean ± s.e.m. are shown in all graphs. n represents number of fins analysed, except in K, where n equals number of cells. BRE:GFP transgene used: BRE:eGFP (Laux et al., 2011).

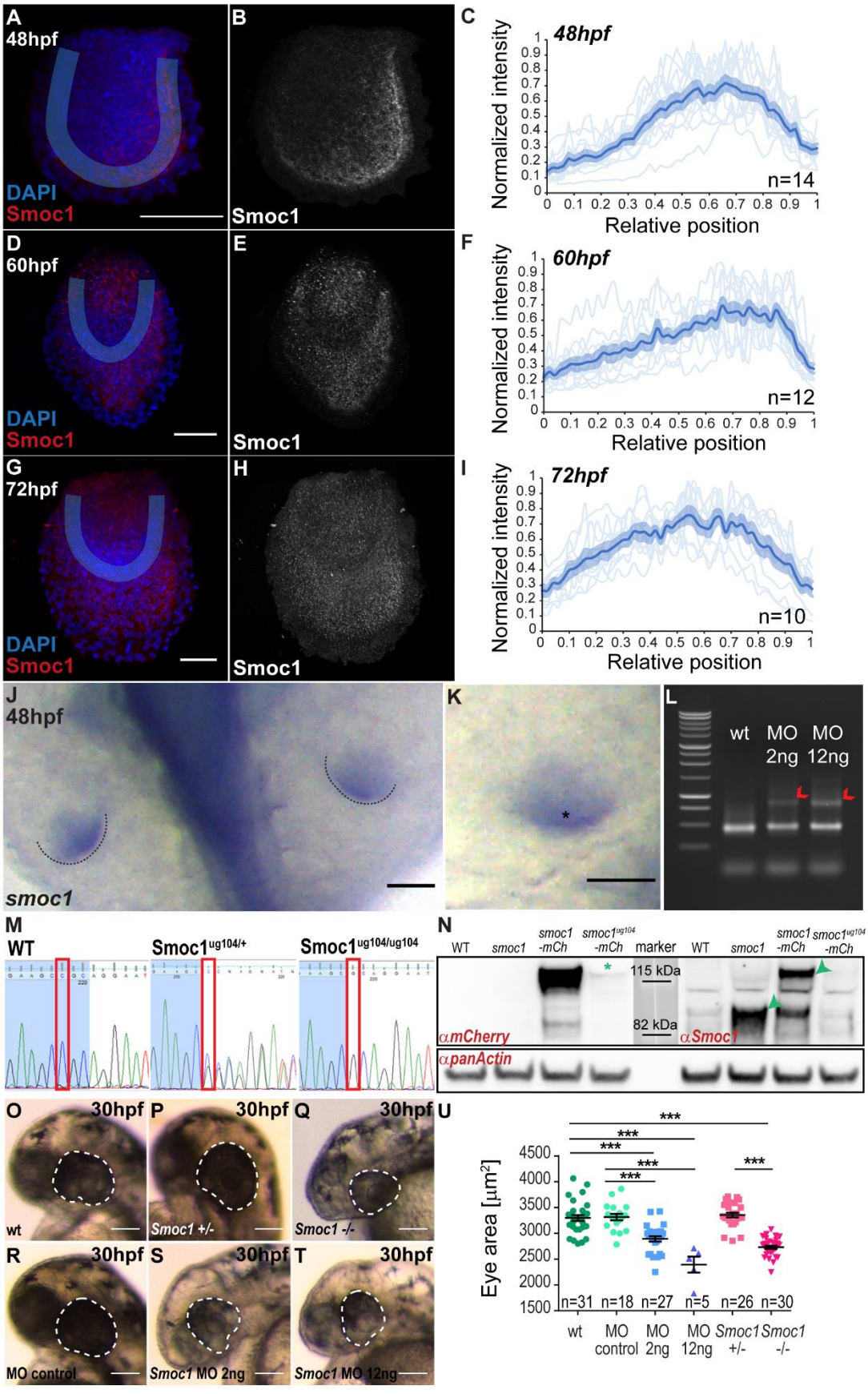
A
48hpf
DAPI
Smoc1
B
Smoc1
C
48hpf
Normalized intensity
Relative position
n=14
D
60hpf
DAPI
Smoc1
E
Smoc1
F
60hpf
Normalized intensity
Relative position
n=12
G
72hpf
DAPI
Smoc1
H
Smoc1
I
72hpf
Normalized intensity
Relative position
n=10
J
48hpf
smoc1
K
L
wt
MO 2ng
MO 12ng
M
WT
Smoc1ug104/+
Smoc1ug104/ug104
N
WT
smoc1
smoc1 -mCh
smoc1ug104 -mCh
marker
115 kDa
82 kDa
αmCherry
αSmoc1
αpanActin
O
30hpf
wt
P
30hpf
Smoc1 +/-
Q
30hpf
Smoc1 -/-
R
30hpf
MO control
S
30hpf
Smoc1 MO 2ng
T
30hpf
Smoc1 MO 12ng
U
Eye area [μm2]
n=31 n=18 n=27 n=5 n=26 n=30
wt
MO control
MO 2ng
MO 12ng
Smoc1 +/-
Smoc1 -/-

Figure S3. Smoc1 expression pattern in the pectoral fin. Related to Figure 4.

A-B, D-E, G-H Smoc1 immunostainings in pectoral fins at different times. Blue area, ROI. **C,F,I** Average intensity of normalized Smoc1 immunostaining signal *versus* relative position (along ROI midline). Light blue, individual profiles; dark blue, mean; shadowing, s.e.m. per relative position, Anterior, left; distal, down. **J-K** *smoc1* transcript pattern in pectoral fins (*in situ* hybridization using antisense probe) at 48 hpf. Dashed line, fin border. Asterisk highlights distal region of higher *smoc1* expression. **L** RT-PCR of cDNA of 24 hpf embryos in different conditions, including wildtype and two different concentrations of the splicing morpholino. Arrowheads, amplicons corresponding to the event of splicing block. **M** Sequences of wildtype, *Smoc1* heterozygotes and *Smoc1* homozygotes. Red box highlights nucleotide affected. **N** Western blots using mCherry (left) and Smoc1 (right) antibodies, performed in extracts from WT embryos and overexpression embryos injected with indicated mRNAs. Green asterisk highlights residual mCherry translation in embryos injected with *smoc1*^{ug104}-mCherry mRNA, which recapitulates the mutation of the CRISPR mutant. Because mCherry is C-terminal, this indicates a low level of read-through across the mutation caused by CRISPR, as previously reported (Schueren and Thoms, 2016). Green arrowheads indicate that the antibody against human Smoc1 recognizes the overexpressed zebrafish Smoc1. Anti-panActin antibody for the loading control. **O-T** Embryos highlighting the eye regions (dash) for different experimental conditions, at 30 hpf. **U** Average eye area for the conditions tested in O-T. For all statistical analyses: ***P<0.0001; two-tailed, unpaired, non-parametric Mann–Whitney tests. Mean ± s.e.m. are shown in all bar graphs. n represents number of fins analysed, except in U, where n equals number of eyes. Scale bars, 50µm.

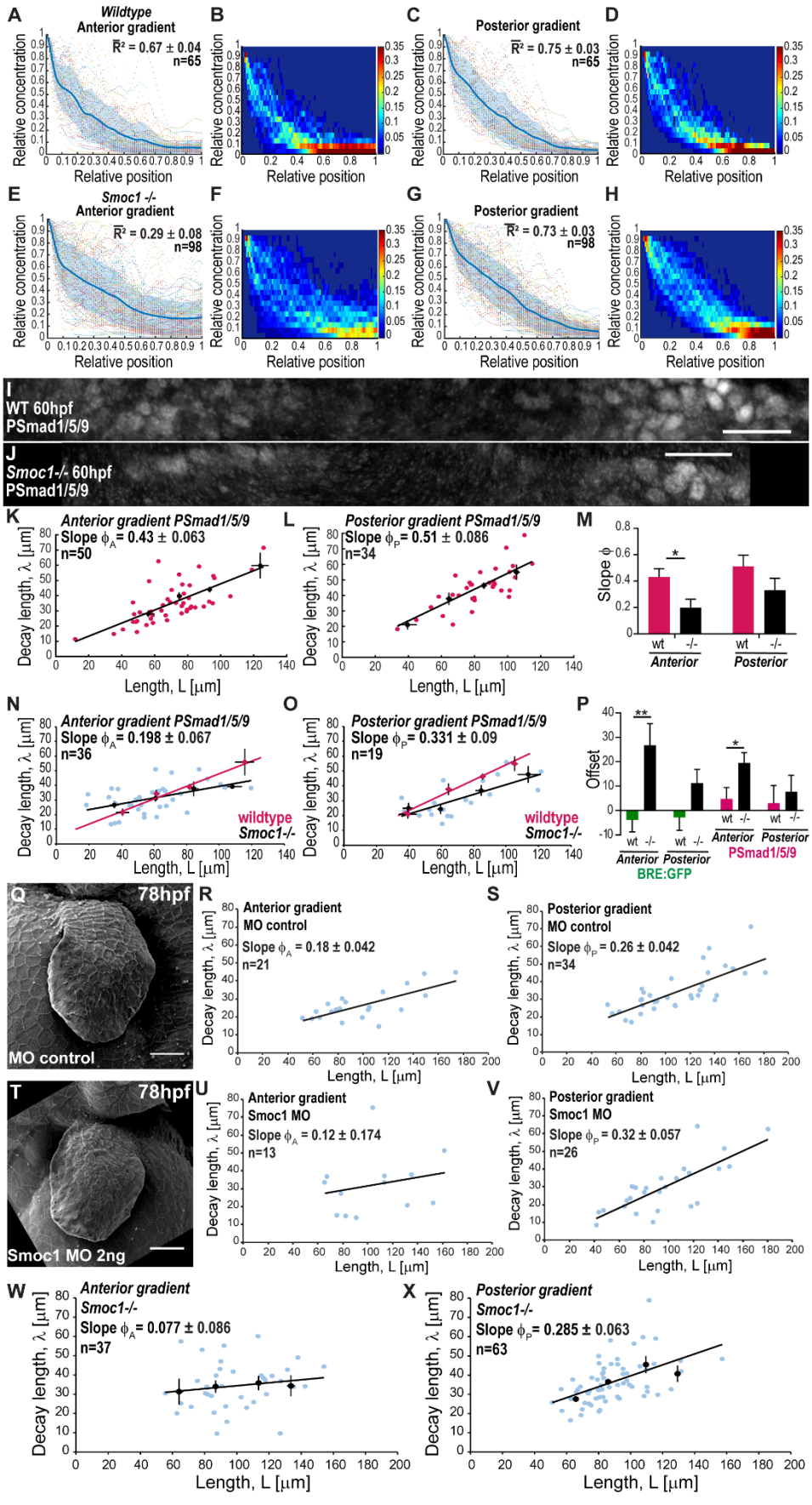
A
Wildtype
Anterior gradient
R² = 0.67 ± 0.04
n=65
B
C
Posterior gradient
R² = 0.75 ± 0.03
n=65
D
E
Smoc1 -/-
Anterior gradient
R² = 0.29 ± 0.08
n=98
F
G
Posterior gradient
R² = 0.73 ± 0.03
n=98
H
Relative concentration
Relative position
I
WT 60hpf
PSmad1/5/9
J
Smoc1-/- 60hpf
PSmad1/5/9
K
Anterior gradient PSmad1/5/9
Slope ϕA = 0.43 ± 0.063
n=50
L
Posterior gradient PSmad1/5/9
Slope ϕP = 0.51 ± 0.086
n=34
M
Slope ϕ
wt
-/-
Anterior
Posterior
Decay length, λ [μm]
Length, L [μm]
N
Anterior gradient PSmad1/5/9
Slope ϕA = 0.198 ± 0.067
n=36
wildtype
Smoc1-/-
O
Posterior gradient PSmad1/5/9
Slope ϕP = 0.331 ± 0.09
n=19
P
Offset
PSmad1/5/9
BRE:GFP
Q
78hpf
MO control
R
Anterior gradient
MO control
Slope ϕA = 0.18 ± 0.042
n=21
S
Posterior gradient
MO control
Slope ϕP = 0.26 ± 0.042
n=34
T
78hpf
Smoc1 MO 2ng
U
Anterior gradient
Smoc1 MO
Slope ϕA = 0.12 ± 0.174
n=13
V
Posterior gradient
Smoc1 MO
Slope ϕP = 0.32 ± 0.057
n=26
W
Anterior gradient
Smoc1-/-
Slope ϕA = 0.077 ± 0.086
n=37
X
Posterior gradient
Smoc1-/-
Slope ϕP = 0.285 ± 0.063
n=63

Figure S4. *Smoc1*^{ug104} mutant and morphants scaling phenotype. Related to Figures 3 and 5.

A-H Gradient collapse analysis. Relative BRE:GFP concentration profiles $C(r,t)/C0(t)$ *versus* relative position in ROI, from 48 to 78 hpf, in wildtype (A, C) and *Smoc1-/-* mutants (E, G). Blue line represents the average curve of the profiles; standard deviation (shadows) per relative position is shown. **B, D, F, H** Density plots of the gradients in A, C, E, F. LUT corresponds to the fraction of normalized gradients passing through a certain bin. Bin size: 0.05 for ordinates and 0.05 for abscissas. **I-J** Phospho-Smad1/5/9 immunostainings showing gradients in *Smoc1* homozygote mutants (J) and wildtype controls (I) displayed as straightened ROI, like in Fig. 1D, at 60 hpf. **K-L** Decay length λ *versus* ROI half-length (L) of Phospho-Smad1/5/9 anterior (K) and posterior (L) wildtype gradients. Pink dots, individual data; black dots, average from length bins ± s.e.m. Lines, linear fits with goodness of fit: ϕ_A R^2=0.50; ϕ_P R^2=0.51. **M** Comparison of slope values, $\phi = \lambda/L$ from Phospho-Smad1/5/9 gradients in wildtype or *Smoc1-/-* conditions. **N-O** Decay length λ *versus* ROI half-length (L) in anterior (N) or posterior (O) Phospho-Smad1/5/9 gradients, in *Smoc1-/-* mutants (black and blue). Blue dots, individual data; black dots, average from length bins ± s.e.m. Black lines, linear fits with goodness of fit: ϕ_A R^2=0.22; ϕ_P R^2=0.48. Pink lines correspond to wildtype data from K-L. **P** Comparison of offsets from linear fits of scaling plots of BRE:GFP (from Fig. 3C-D, Fig. 5D-E) or Phospho-Smad1/5/9 (from K-L, N-O) gradients in wildtype and Smoc1-/- mutants. **Q-V** Gradient analysis in *smoc1* morphants. **Q,T** SEM images of pectoral fins of larvae injected with control morpholino (Q) or the *smoc1* splicing morpholino (T). Anterior on the left, distal down. **R-S, U-V** Decay length, λ, versus ROI half-length (L), in control morphants (R-S) or *smoc1* morphants (U-V). Lines, linear fits with goodness of fit: in controls ϕ_A R^2=0.53; ϕ_P R^2=0.56; *smoc1* morphants ϕ_A R^2=0.05; ϕ_P R^2=0.59. Note that the s.e.m. for the slope of the anterior *smoc1* morphant gradient is compatible with abolished scaling (slope $= 0$). **W-X** Decay length λ *versus* ROI half-length (L) in anterior (W) or posterior (X) BRE:GFP gradients of *Smoc1-/-* mutants (Figure 5C-D with individual data); Lines, linear fits with goodness of fit: ϕ_A R^2=0.02; ϕ_P R^2=0.26. In all scaling plots: slope (ϕ) values ± s.e.m. are shown. Mean ± s.e.m. are shown in all bar graphs. n represents number of fins analysed. For all statistical analyses: **P<0.01, *P<0.05; two-tailed, unpaired, non-parametric Mann–Whitney tests. BRE:GFP transgene used: BRE:eGFP (Laux et al., 2011). Scale bars: 20µm (I, J), 50µm (Q,T).

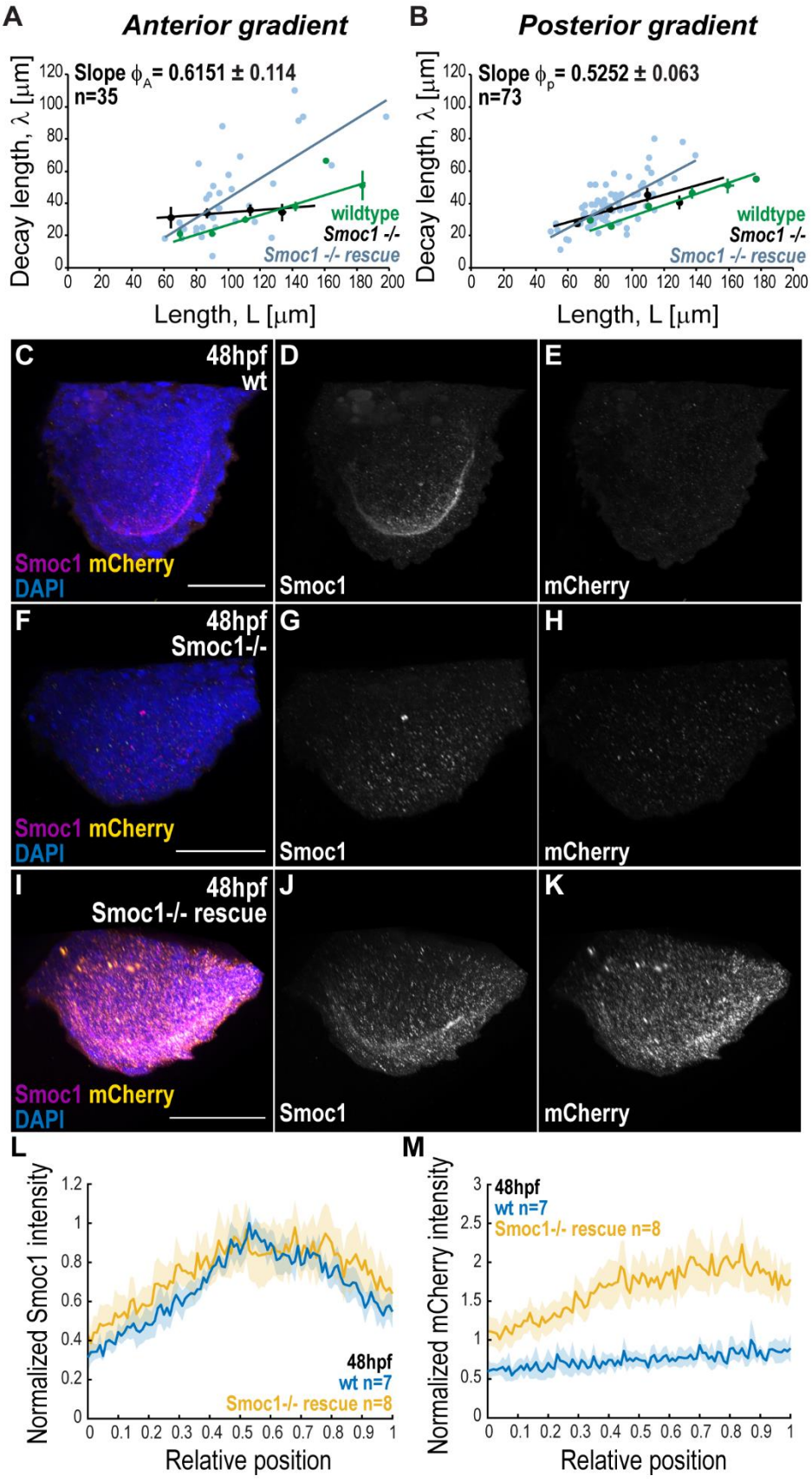
A
Anterior gradient
Slope ϕ_A = 0.6151 ± 0.114
n=35
Decay length, λ [μm]
Length, L [μm]
wildtype
Smoc1 -/-
Smoc1 -/- rescue
B
Posterior gradient
Slope ϕ_p = 0.5252 ± 0.063
n=73
Decay length, λ [μm]
Length, L [μm]
wildtype
Smoc1 -/-
Smoc1 -/- rescue
C
48hpf
wt
Smoc1 mCherry
DAPI
D
Smoc1
E
mCherry
F
48hpf
Smoc1-/-
Smoc1 mCherry
DAPI
G
Smoc1
H
mCherry
I
48hpf
Smoc1-/- rescue
Smoc1 mCherry
DAPI
J
Smoc1
K
mCherry
L
Normalized Smoc1 intensity
Relative position
48hpf
wt n=7
Smoc1-/- rescue n=8
M
Normalized mCherry intensity
Relative position
48hpf
wt n=7
Smoc1-/- rescue n=8

Figure S5. Smoc1^{ug104} mutant rescue leads to gradient over-scaling. Related to Figure 5.
A-B Decay length λ *versus* ROI half-length (L) in anterior (A) or posterior (B) gradients of *Smoc1-/-* mutants injected with 20pg *smoc1* mRNA (rescue; blue fit lines and dots). Slope (ϕ) values for rescue ± s.e.m. are shown. Lines, linear fits with goodness of fit: *Smoc1-/-* rescue ϕ_A R^2=0.49; ϕ_P R^2=0.51. Green corresponds to wildtype data from Fig. 3C-D; black represents *Smoc1-/-* data from Fig. 5D-E. BRE:GFP transgene used: BRE:eGFP (Laux et al., 2011). **C-K** Smoc1 (magenta) and mCherry (yellow) immunostaining expression in wildtype (C-E), *Smoc1-/-* mutants (F-H) or in *Smoc1-/-* mutants injected with 20pg of *smoc1-mCherry* mRNA (*rescue*) (I-K), at 48 hpf. Anterior on the left, distal down. **L-M** Average intensity of normalized Smoc1 (L) or mCherry (M) immunostainings *versus* relative position (ROI midline) in wildtype (blue), or Smoc1-/- mutants injected with 20pg *smoc1-mCherry* mRNA (rescue, yellow). Intensities were normalized to the wildtype maxima for comparison. Shadowing corresponds to s.e.m. per relative position. n represents number of fins analysed. Scale bars, 50µm.

Supplemental Data

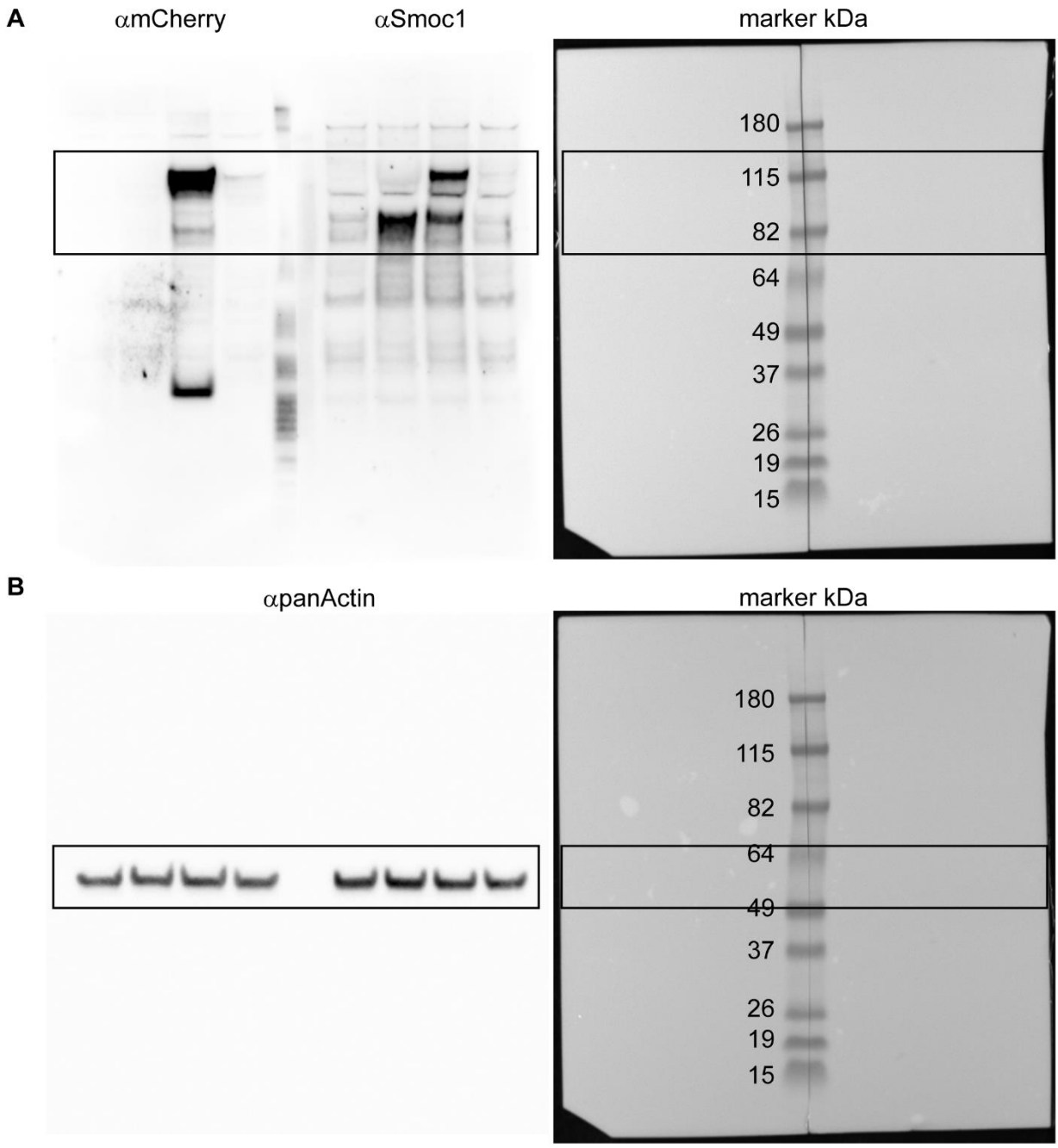

Data S1. Western blot source data. Related to STAR Methods and Fig. S3N.
Uncropped scans with size marker indications for Fig. S3N. **A** Uncropped scans of anti-mCherry and anti-Smoc1 blots. **B** Uncropped scan of loading control anti-panActin.

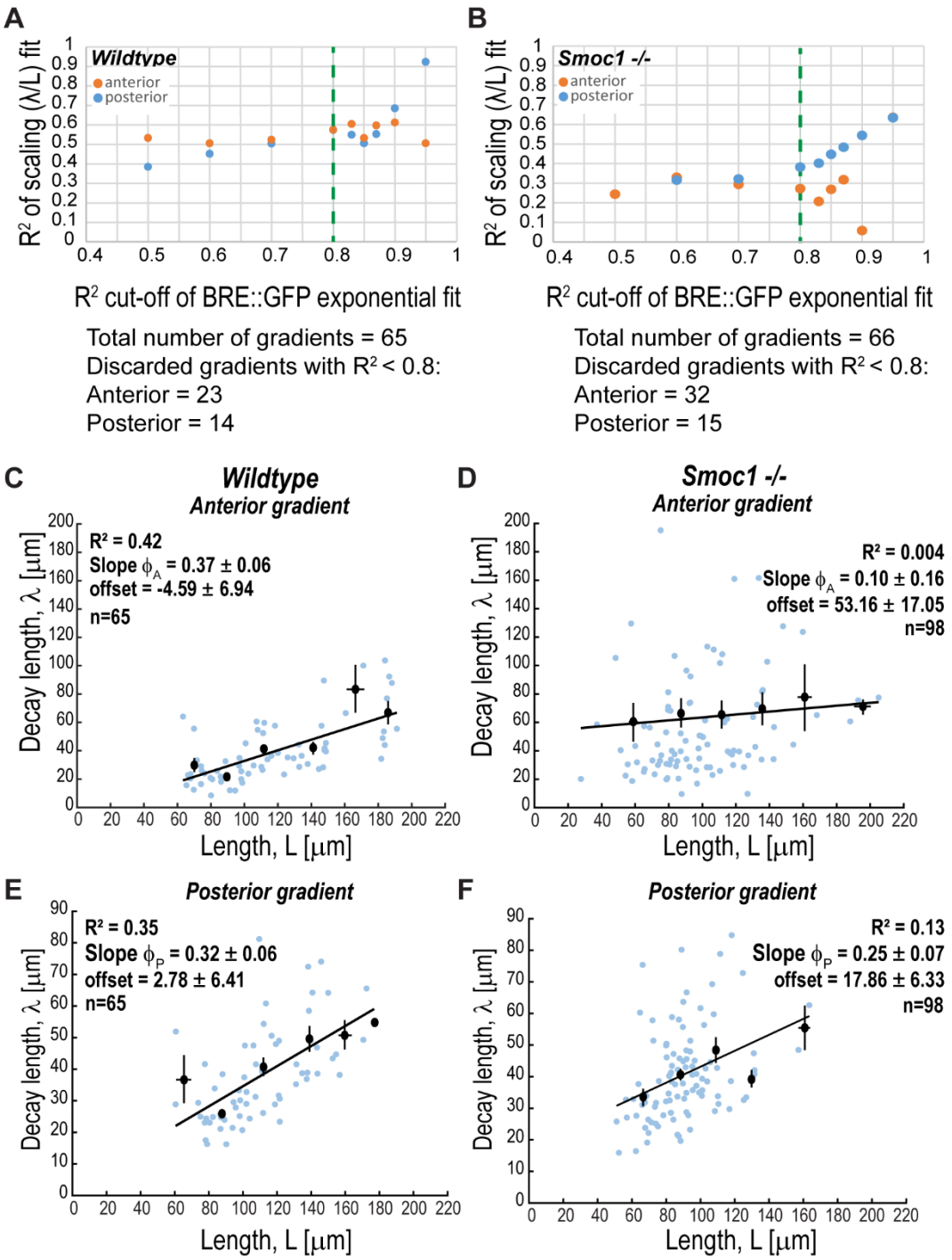

Data S2. Scaling of BMP signalling gradients (full datasets). Related to STAR Methods and to Figs. 3, 5, S4, S5.

A-B R^2 statistical analysis of BRE:GFP gradients. R^2 values obtained from linear fits in scaling plots (decay length, λ, *vs.* fin length, L) *versus* R^2 cut-off of individual BRE:GFP exponential fits, in wildtype (A) or *Smoc1-/-* mutants (B). Dashed lines, R^2 cut-off in which the quality of the scaling

plot fit improves considerably. Based on this, we considered for the scaling plot analysis only the profiles whose exponential gradients presented $R^2 \geq 0.8$. The estimation of decay length from fits with $R^2 < 0.8$ is likely to be inaccurate. **C-E** Decay length versus ROI half-length (L) in wildtype (C, E) and *Smoc1* homozygote mutants (D, F). Black lines, linear fits to individual data, with goodness of fit, R^2. Black dots, average from length bins ± s.e.m. Slope (ϕ) and offset values ± s.e.m. are shown. n represents number of fins analysed. BRE:GFP transgene used: BRE:eGFP (Laux et al., 2011).

Methods S1. Theoretical Framework. Related to Figs. 3, 5, S3, S4, S5.

1. Growth control and gradient scaling in two-dimensional geometries; 2. Amplitude power-law and growth control by relative time derivative of signaling; 3. Theory for ubiquitous expression of *smoc1*.

1. Growth control and gradient scaling in two dimensional geometries

I. HOMOGENEOUS AND ANISOTROPIC TISSUE GROWTH

We consider a tissue in three dimensions described by a coordinate system with the x-axis along the proximal-distal (PD) axis, the y-axis along the anterior-posterior (AP) axis and the z-axis along the dorsal-ventral (DV) axis. We discuss tissue growth that is is homogeneous and anisotropic and focus on the simple case where no growth occurs along the z-axis. The tissue size is characterized by the extensions along the main axies: L_x denotes the tissue size along the PD axis, L_y the size along the AP axis and L_z along the DV axis.

The area growth rate is

$$g = \frac{\dot{A}}{A} \tag{1}$$

The area growth rate can also be written as

$$g = \frac{\dot{L}_x}{L_x} + \frac{\dot{L}_y}{L_y} \tag{2}$$

where the dot denotes a time derivative. For homogeneous isotropic growth in the x-y plane, the cell velocity field is given by

$$v_x = \frac{g}{1+\epsilon} x \tag{3}$$

$$v_y = \frac{g\epsilon}{1+\epsilon} y \tag{4}$$

Here ϵ characterizes the growth anisotropy. For $\epsilon = 1$ growth is isotropic, for $\epsilon = 0$ growth is solely along the x-axis and in the limit of large ϵ growth is solely along the y-axis. The rates of change of tissue size then obey

$$\dot{L}_x = \frac{g}{1+\epsilon} L_x \tag{5}$$

$$\dot{L}_y = \frac{g\epsilon}{1+\epsilon} L_y \tag{6}$$

If ϵ is constant, the tissue sizes then scale as $L_x \sim L_y^{1/\epsilon}$.

II. GROWTH CONTROL BY RELATIVE RATES OF CONCENTRATION INCREASE

We have recently proposed a general principle of growth control based on the idea that increases in growth factor or morphogen levels stimulate growth at a rate that is proportional

to the relative rate of increase in concentration (Wartlick et al., 2011, 2014). A given cell uses receptors on its surface and a signaling pathway to detect changes in the concentration $c_{\text{cell}} = c(x_{\text{cell}}, y_{\text{cell}})$ at the position $(x, y) = (x_{\text{cell}}, y_{\text{cell}})$ of the cell. Here $c(x, y)$ is the morphogen concentration profile in space of a growth factor.

The growth at a rate g is generated as signaling output of the system with

$$g = \beta^{-1} \frac{\dot{c}_{\text{cell}}}{c_{\text{cell}}} \tag{7}$$

where

$$\dot{c}_{\text{cell}} = \partial_t c(x, y, t) + \mathbf{v} \cdot \nabla c(x, y, t) \tag{8}$$

is obtained using a time derivative in the reference frame that moves with the cells at velocity $\mathbf{v} = (v_x, v_y)$. It was shown before in a simpler case of one dimensional gradients that growth resulting from this growth control rule is spatially homogeneous if morphogen profiles scale (Wartlick et al., 2011, 2014).

III. SCALING OF THE MORPHOGEN PROFILE

We consider a morphogen profile that varies along the x axis only. Scaling of the morphogen profiles implies that if the tissue length L_x is rescaled by the tissue extension in x direction, the shape of the profile is not changed but the overall amplitude can be time-dependent. Scaling of the morphogen profile implies that it can be written as

$$c(x, y, t) = C_0(t)\, \Xi\left(\frac{x}{L_x(t)}\right) \tag{9}$$

Here $C_0(t)$ is the time dependent amplitude and the shape function $\Xi(r_x)$ with $r_x = x/L_x$ is independent of time. If the profile c scales and growth is homogeneous, we have $\dot{c}_{\text{cell}} = \dot{C}_0$. In this case the growth rate becomes

$$g = \beta^{-1} \frac{\dot{C}_0}{C_0} \tag{10}$$

independent of position in the three dimensional tissue.

If the amplitude $C_0(t)$ increases with system size as a power law with exponent q, we have

$$C_0 \sim L_x^q \sim L_y^{q/\epsilon} \tag{11}$$

we then find

$$\frac{\dot{C}_0}{C_0} = q\frac{\dot{L}_x}{L_x} = \frac{q}{\epsilon}\frac{\dot{L}_y}{L_y} \tag{12}$$

Using Eq. (2) we then have

$$g = \frac{1+\epsilon}{q}\frac{\dot{C}_0}{C_0} \tag{13}$$

This is consistent with the growth rule if $\beta = q/(1+\epsilon)$. Thus the signature of homogeneous growth due to a scaling morphogen profile is that the amplitude $C_0(t)$ increases with system size with an exponent q.

A. Scaling in the pectoral fin of the zebrafish

In order to test whether the profiles $c(x, y, t)$ observed in the fin actually scale during growth, we consider concentration profiles along the center line of a curved region of interest (ROI). The centerline shape can be defined as a time independent scaling function $y = L_y f(x/L_x)$ which for given value of x provides the y coordinate of the ROI centerline. We then consider the linear profiles along the ROI centerline

$$c_x(x,t) \;=\; c(x, L_y f(x/L_x)) \tag{14}$$

$$c_y(y,t) \;=\; c(L_x f^{-1}(y/L_y), y) \tag{15}$$

where f^{-1} denotes the inverse of the function f. If the profiles $c(x, y, t)$ scale, then

$$c_x(x,t) \;=\; C_0(t)\xi(x/L_x) \tag{16}$$

$$c_y(y,t) \;=\; C_0(t)\xi(f^{-1}(y/L_y)) \tag{17}$$

and the normalized profiles $c_x/C_0 = \xi(r_x)$ and $c_y/C_0 = \xi(f^{-1}(r_y))$ collapse each on a single curve. Fitting exponential functions $c_x/C_0 \simeq \exp(-r_x/\bar{\lambda}_x)$ and $c_y/C_0 \simeq \exp(-r_y/\bar{\lambda}_y)$ with fit parameters $\bar{\lambda}_x$ and $\bar{\lambda}_y$ to these collapsed profiles provides the scaling of decay lengths in x and y directions with system sizes $\lambda_x \simeq \bar{\lambda}_x L_x$ and $\lambda_y \simeq \bar{\lambda}_y L_y$.

IV. GROWTH CONTROL AND GRADIENT SCALING IN TWO DIMENSIONS

We consider a morphogen that is secreted within a localized source, diffuses isotropically and is degraded

$$\partial_t c + v_x\partial_x c + v_y\partial_y c = D\partial_x^2 c + D\partial_y^2 c - (k+g)c + s(x) = 0 \tag{18}$$

Here k denotes the degradation rate and D is a diffusion coefficient. Here the source is a stripe along the y-axis with $s(x) = \nu\theta(w_x - x)\theta(w_x + x)$, where w_x is the half source width and θ denotes the Heavyside function. We consider growth regulated by relative changes of concentration perceived by a cell in the dynamic tissue

$$g = \frac{1}{\beta}\frac{\partial_t c + v_x\partial_x c + v_y\partial_y c}{c} \tag{19}$$

If growth is homogeneous, the velocity fields are

$$v_x = \frac{g}{1+\epsilon}x \tag{20}$$

$$v_y = \frac{g\epsilon}{1+\epsilon}y \tag{21}$$

The system sizes in x was and y directions grow as

$$\dot{L}_x = \frac{g}{1+\epsilon}L_x \tag{22}$$

$$\dot{L}_y = \frac{g\epsilon}{1+\epsilon}L_y \tag{23}$$

We are looking for solutions to the dynamic equations with homogeneous growth that scale with system size

$$c(x, y, t) = C_0(t)\xi(\frac{x}{L_x}) \tag{24}$$

We thus have

$$0 = \frac{D}{L_x^2}\partial_{r_x}^2\xi(r_x, r_y) - (k + g(1+\beta))\xi(r_x) + s(r_x)/C_0(t) \tag{25}$$

where $r_x = x/L_x$. We can also write this as

$$0 = \partial_{r_x}^2\xi - \frac{k_g L_x^2}{D}\xi + \frac{sL_x^2}{DC_0} \tag{26}$$

where $k_g = k + g(1+\beta)$. Scaling solutions exist for $C_0 \sim L_x^2$ and $k_g \sim L_x^{-2}$. We thus find the solutions

$$c(x,t) = \frac{\nu}{k + g(1+\beta)}\left(1 - \frac{\sinh(L_x/\lambda - w_x/\lambda))}{\sinh(L_x\lambda)}\right)\cosh(x/\lambda) \tag{27}$$

for $x < w_x$, and

$$c(x,t) = \frac{\nu}{k + g(1+\beta)}\frac{\sinh(w_x/\lambda))}{\sinh(L_x\lambda)}\cosh((L_x - x)/\lambda) \tag{28}$$

for $x > w$, where

$$\lambda = \left(\frac{D}{k + g(1+\beta)}\right)^{1/2} \quad . \tag{29}$$

We thus have $C_0 \sim \nu/(k + g(1 + \beta))$. The growth law implies $\beta g = d \log C_0/dt$. Since we also have $g = (1 + \epsilon) d \log L_x/dt$ and $C_0 \sim L_x^2$, scaling solutions exist for a specific value of $\beta = \beta_c$ with $\beta_c = 2/(1 + \epsilon)$.

2. Amplitude power-law and growth control by relative time derivative of signalling

Below is a summary of some theoretical considerations discussed in previous reports (Aguilar-Hidalgo et al., 2018; Wartlick et al., 2011, 2014), which are relevant to this work and presented here for convenience. We find an empirical power-law relationship between the gradient amplitude and the length of the organ as $C_0 \sim {L_x}^q$, with L_x the tissue length along the x axis. Because of scaling, the concentration of the morphogen in any cell in the tissue remains proportional to the amplitude, $C_0 \sim C_{cell}$ and therefore also $C_{cell} \sim {L_x}^q$. The time derivative of this expression gives $g_x = \frac{1}{q}\frac{\dot{C}_{cell}}{C_{cell}}$, with g_x the linear growth rate along the x axis, i.e. $g_x = \frac{\dot{L}_x}{L_x}$; and $\dot{C}_{cell}$ the time derivative of morphogen concentration in a cell. Considering a constant growth anisotropy $\varepsilon = g_y/g_x$, then the area growth rate is $g = g_x + g_y = (1 + \varepsilon) g_x$. Therefore $g = \frac{(1+\varepsilon)}{q}\frac{\dot{C}_{cell}}{C_{cell}}$.

To calculate the relative increase in cellular morphogen concentration $\alpha = \Delta C_{cell}/C_{cell}$ during a cell cycle of duration θ, we approximate $\dot{C}_{cell} \approx \Delta C_{cell}/\theta$ and $\theta \approx log(2)/g$. These approximations are fair, since $\dot{C}_{cell}$ and g change in time scales which are longer than θ. We then plug these approximations in the g equation above to obtain $\frac{log(2)}{\theta} = \frac{1+\varepsilon}{q}\frac{\Delta C_{cell}/\theta}{C_{cell}}$, from where $\alpha = \Delta C_{cell}/C_{cell} \approx log(2)\frac{q}{(1+\varepsilon)}$. In the fin bud, with $q = 0.9$ and $\varepsilon = 0.65$, then $\alpha = 0.38$. Therefore, fin cells divide when their BMP signaling levels increase by 38% from the beginning of the cell cycle.

3. Theory for ubiquitous expression of *smoc1*

In the main text, we showed that in Smoc1-/- mutants injected with *smoc1* mRNA, the gradient length scale expands as the tissue grows and appears to scale. The scaling factor in this experiment was larger than the one in control fins (Fig. 5F and Fig. S5A-B). In

this section we develop a theoretical framework within which to interpret these observations. Our logic is based on the assumption that Smoc1 acts as an expander of the morphogen by repressing its degradation as proposed in the expander-repression model by (Ben-Zvi, D. and Barkai, 2010). In the original expander-repression model, the expander forms an approximately flat profile and accumulates in the tissue over time because its production is repressed by the morphogen, it diffuses very fast and its degradation is negligible. Here, we show that this mRNA overexpression experiment recapitulates the circumstances of an expander-repression circuit.

Let us consider an expander molecule, E, that is transcribed everywhere in a tissue. The dynamics of E are then described by,

$$D_t E = \nabla(D_E \nabla E) - (k_E + g)E + s_E \tag{30}$$

Where D_E is the diffusion coefficient of E, k_E is the degradation rate of E, g is the tissue growth rate and s_E is the source term that captures the production rate of E. For the purposes of our analysis we assume that the diffusion coefficient is very large so that the expander is uniform in space. Under these conditions Eq. (30) can be rewritten as,

$$\partial_t E_0(t) = \frac{1}{L}\int_0^L \left[-(k_E + g)E_0(t) + s_E\right]\, dx \tag{31}$$

We can evaluate the integral on the RHS to obtain,

$$\partial_t E_0(t) = -(k_E + g)E_0(t) + \frac{w_E\ \nu_E}{L} \tag{32}$$

Where $E_0(t) = E(0,t)$. We can integrate Eq. (32) and use $E_0(t) = 0$ to obtain the following expression for the time dependent concentration of $E_0(t)$,

$$E_0(t) = \frac{w_E \nu_E}{L(k_E + g)}\left(1 - e^{-(k_E+g)t}\right) \tag{33}$$

For small $(k_E + g)$ we can use the approximation $e^{-(k_E+g)t} \approx 1 - (k_E + g)t$ which leads to,

$$E_0(t) = \frac{w_E \nu_E t}{L} \tag{34}$$

Following the original expander-repression model (Ben-Zvi, D. and Barkai, 2010), we assume that the expander degradation is negligible. At the same time, the growth rate in our system is very slow. It follows that Eq. (34) is approximately true. We are further assuming that

the expander is produced everywhere in the tissue (the mRNA is ubiquitously expressed) so $w_E = L$ and Eq. (34) reduces to,

$$E_0(t) = \nu_E t \tag{35}$$

It follows that the concentration of the expander accumulates over time. According to the expansion-repression model, the morphogen degradation rate, k , is regulated by the expander so that k decreases as the expander accumulates. We can therefore write the time dependent decay length of the morphogen as,

$$\lambda = \sqrt{\frac{D}{k(E_0(t))}} \tag{36}$$

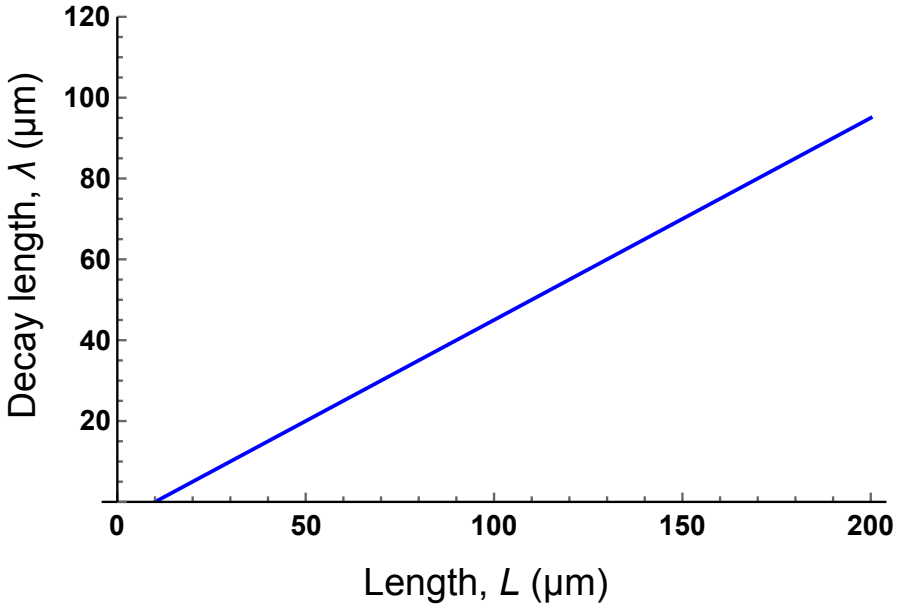

Methods Image 1. Theory of apparent scaling due to mRNA injection. The blue line shows the relationship $\lambda = \sqrt{\frac{D}{A}}\frac{\nu_E}{v}\left[L(t) - \hat{L}\right]$ for $\sqrt{\frac{D}{A}}\frac{\nu_E}{v} = 0.5$ and $\hat{L} = 10\mu$m.

At the same time, the embryo grows continuously during development so that its size is an increasing function of time, $L(t)$ (and therefore time is an increasing function of length, $t(L)$). It follows that λ becomes an increasing function of size which could in principle lead to the expansion of the gradient over time and approximate scale (as observed in the experiments). Methods Image 1 shows the predicted decay length versus size for a particular case where $k = \frac{A}{E_0(t)^2}$ and $L(t) = \hat{L} + vt$ for some constants A, $\hat{L}$ and v. In principle, qualitatively similar results are expected for other choices for the functions $k(E_0(t))$ and $L(t)$ as long as k

remains a decreasing function of the expander concentration and L is an increasing function of time.

In summary, we show that overexpressing *smoc1* by mRNA injection leads to the accumulation of the expander over time and could in principle scale the gradient. The dynamics of increasing expander concentration is in accordance with the expander-repression theory proposed by (Ben-Zvi, D. and Barkai, 2010). Much like in the expander-repression model, the mRNA injection leads to an increased concentration of the expander with the size of the tissue. This is expected to expand the gradient as the tissue grows since the expander suppresses the degradation of the morphogen.